Journal of Ultrasound (2022) 25:121–128
https://doi.org/10.1007/s40477-021-00569-9

TECHNICAL REPORTS

Relationship between the overall survival in glioblastomas and the radiomic features of intraoperative ultrasound: a feasibility study

Santiago Cepeda[1] · Sergio García-García[1] · Ignacio Arrese[1] · María Velasco-Casares[2] · Rosario Sarabia[1]

Received: 18 December 2020 / Accepted: 4 February 2021 / Published online: 16 February 2021
© Società Italiana di Ultrasonologia in Medicina e Biologia (SIUMB) 2021

Abstract

Purpose Predicting the survival of patients diagnosed with glioblastoma (GBM) is essential to guide surgical strategy and subsequent adjuvant therapies. Intraoperative ultrasound (IOUS) can contain biological information that could be correlated with overall survival (OS). We propose a simple extraction method and radiomic feature analysis based on IOUS imaging to estimate OS in GBM patients.

Methods A retrospective study of surgically treated glioblastomas between March 2018 and November 2019 was performed. Patients with IOUS B-mode and strain elastography were included. After preprocessing, segmentation and extraction of radiomic features were performed with LIFEx software. An evaluation of semantic segmentation was carried out using the Dice similarity coefficient (DSC). Using univariate correlations, radiomic features associated with OS were selected. Subsequently, survival analysis was conducted using Cox univariate regression and Kaplan–Meier curves.

Results Sixteen patients were available for analysis. The DSC revealed excellent agreement for the segmentation of the tumour region. Of the 52 radiomic features, two texture features from B-mode (conventional mean and the grey-level zone length matrix/short-zone low grey-level emphasis [GLZLM_SZLGE]) and one texture feature from strain elastography (grey-level zone length matrix/long-zone high grey-level emphasis [GLZLM_LZHGE]) were significantly associated with OS. After establishing a cut-off point of the statistically significant radiomic features, we allocated patients in high- and low-risk groups. Kaplan–Meier curves revealed significant differences in OS.

Conclusion IOUS-based quantitative texture analysis in glioblastomas is feasible. Radiomic tumour region characteristics in B-mode and elastography appear to be significantly associated with OS.

Keywords Intraoperative ultrasound · Elastography · Radiomics · Texture · Glioblastoma · Brain tumor

Introduction

Glioblastomas account for approximately 80% of all brain neoplasms. The overall survival (OS) is estimated to be around 15 months despite continuous efforts to find new and more effective treatments [1]. For this reason, one strategy to optimise the therapeutic approach would advocate for adapting the extent of resection and adjuvant therapies of patients to their specific life expectancy.

Nowadays, the union of radiomics and artificial intelligence seeks to establish tumour patterns by analysing preoperative magnetic resonance images (MRI) and correlating the radiomic features with OS [2, 3].

Intraoperative ultrasound (IOUS) has proven to be a handy tool for guiding tumour resection [4]. Advanced modalities, such as contrast-enhanced ultrasound (CEUS),

✉ Santiago Cepeda
cepeda_santiago@hotmail.com

Sergio García-García
segarciagarc@saludcastillayleon.es

Ignacio Arrese
iarreser@saludcastillayleon.es

María Velasco-Casares
mvelascoca@saludcastillayleon.es

Rosario Sarabia
rsarabia@saludcastillayleon.es

[1] Department of Neurosurgery, University Hospital Río Hortega, Calle Dulzaina, 2, 47012 Valladolid, Spain

[2] Department of Radiology, University Hospital Río Hortega, Calle Dulzaina, 2, 47012 Valladolid, Spain

intraoperative ultrasound elastography (IOUS-E), and navigated three-dimensional (3D) ultrasound (US), currently make it possible to exploit the full potential of this versatile and low-cost imaging technique to achieve maximal safe tumour resections [5–11].

IOUS-E is an ultrasound modality that allows in vivo analysis of the elasticity of tissues. It has been used for several years in liver, breast, and thyroid pathology [12–14]. IOUS-E application in neuro-oncology is relatively new. Several publications highlight its advantages and propose a histological correlation [15, 16].

We hypothesise that IOUS images in both B-mode and strain elastography can show tumour texture features correlated with OS in glioblastomas.

Methods

A retrospective analysis of patients who underwent surgery from March 2018 to November 2019 and had a confirmed histopathological diagnosis of glioblastoma was performed. Cases with IOUS studies were included. Only cases in which a gross total resection was achieved, followed by the Stupp protocol treatment, were included [17]. The primary endpoint was overall survival (OS), which was defined as the number of days from the initial pathological diagnosis to death (censored = 1) or the last date that they were known to be alive (censored = 0). Stereotactic biopsies, partial or subtotal resections, tumour recurrence, and patients who could not complete the adjuvant treatment were excluded.

Image acquisition and processing

The US equipment was the Hitachi Noblus model with a C42 probe at a frequency range of 4–8 MHz, scan width of 20 mm radius, and 80° field-of-view (FOV) scan angle. The acquisition of IOUS images was carried out following the methods detailed in previous publications [16, 18]. Ultrasound images were acquired after craniotomy and before dural opening. The ultrasound probe was protected with sterile sheets and positioned perpendicularly over the dura. First, we localised the tumour and the peritumoural areas using B-mode. Then the images were acquired in elastography mode. Compressions were performed over the dura, with the goal of maintaining a constant rhythm and intensity. Manual compression amplitudes and cycle speeds may influence the quality of the elastograms. Too fast compression cycle resulted in poor image quality. Larger-amplitude compressions appeared to produce elastograms demonstrating less strain contrast between the brain and the tumour tissue but more strain at their boundary. Lower-amplitude compressions resulted in images showing better stiffness contrast. When slower palpations were applied, tumour heterogeneity was far more obvious on the elastograms. In addition, the strain propagated far deeper, improving the image definition in deep tissue. Therefore, the optimal parameters seemed to be a compression cycle of 0.5 s and axial displacement of no more than 5 mm. One way to verify that compressions meet these frequency and amplitude criteria is through the representation of the compression waves shown by the equipment (Fig. 1).

Strain ultrasound generates colour maps in real time translucently superimposed on the conventional B-mode images. These images, called elastograms, were acquired in different projections with the intention to cover the tumour, the adjacent parenchyma with signal alteration, and the apparently healthy brain. The colorimetric scale of these images assigns a value ranging from 0 to 256, with 0 (soft) corresponding to red and 256 (hard) corresponding to blue.

The images in B-mode and strain elastography acquired concurrently were stored in 8-bit Tagged Image File Format (TIFF). In each case, one slice was chosen, in which the largest diameter of the tumour was shown. The images were cropped, leaving only the area containing the tumour. Later, the image was rescaled to a size of 512 × 512 pixels. The elastogram images were converted to hue-saturation-brightness (HSB) format, extracting the hue component in which the elasticity was expressed in greyscale. ImageJ software version 1.50i (National Institutes of Health, Maryland, USA) was used for this process (Fig. 2a–c).

Afterward, the B-mode image was used to manually segment the tumour and peritumoural region. We used the open-source program LIFEx version 6.0 (http://www.lifexsoft.org) [19]. Segmentation of the area corresponding to the tumour was performed, avoiding cystic/necrotic regions. The peritumoural area with evidently altered echogenicity was also segmented (Fig. 2d). These regions of interest (ROIs) were saved and exported to be used over the elastograms. The segmentations were performed by a neurosurgeon specially trained in the acquisition of intraoperative ultrasound images and supervised by a senior neuroradiologist.

Evaluation of semantic segmentation and radiomic features extraction

The Dice similarity coefficient (DSC) [20] was used as a metric to evaluate the semantic segmentation of the two regions: tumour and peritumoural area. Segmentations labelled as 'ground truth' were compared with the ROIs drawn by three other neurosurgeons, all of whom had extensive neuroimaging and tumour pathology experience.

The DSC can be defined by the formula $QS = \frac{2C}{A+B} = \frac{2|A \cap B|}{|A|+|B|}$, in which A is the number of pixels of the reference or 'ground truth' ROI, B is the number of

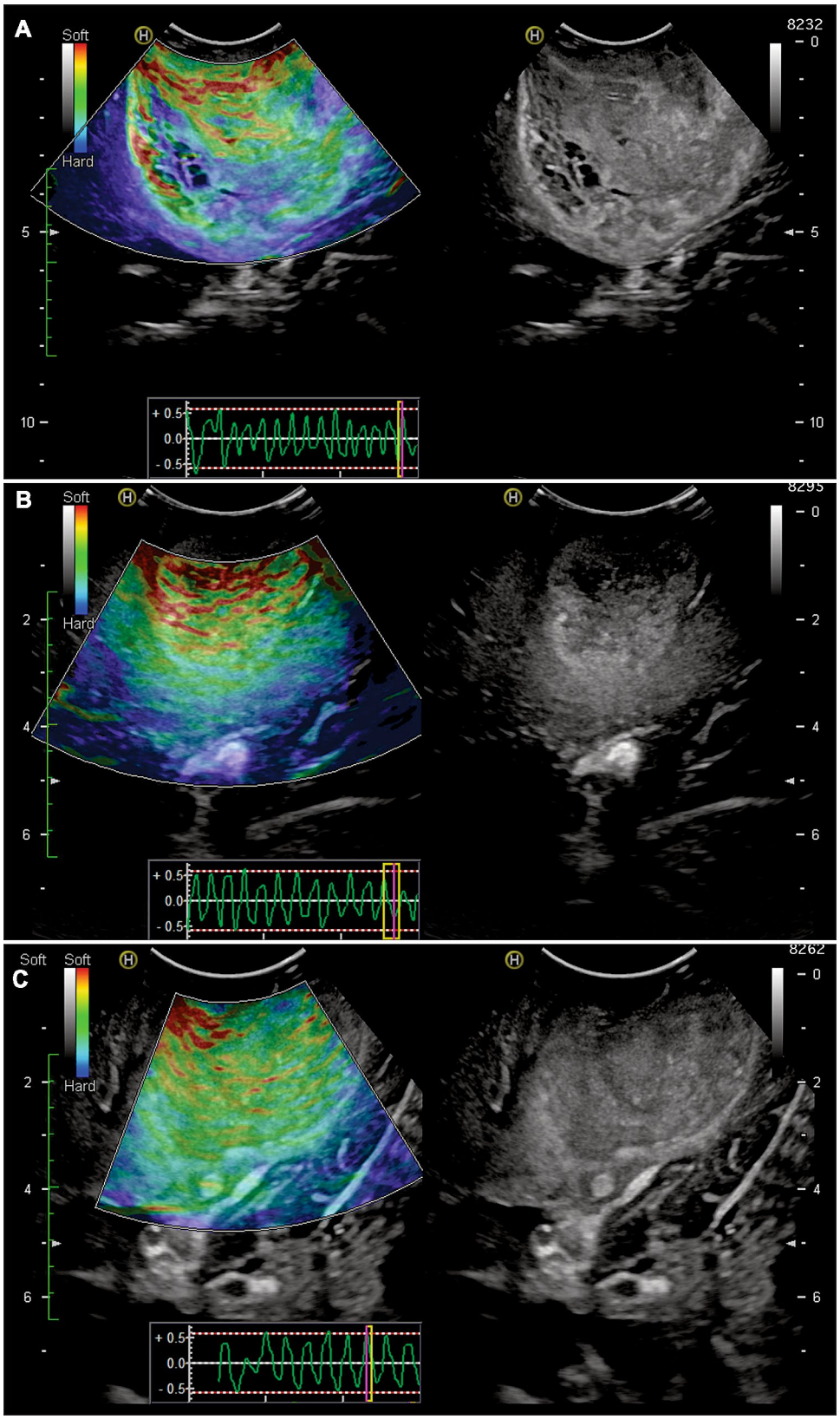

Fig. 1 Illustrative cases of intraoperative ultrasound images and the acquisition technique. Elastograms are shown on the left of the figure, while images acquired in B-mode simultaneously are shown on the right. In the lower part of the elastograms, the schematic representation of the compression waves is observed on a dimensionless scale. **a** A 55-year-old man with right parietal GBM. **b** A 64-year-old woman with a right parietal GBM. **c** A 68-year-old man with a right temporoparietal GBM

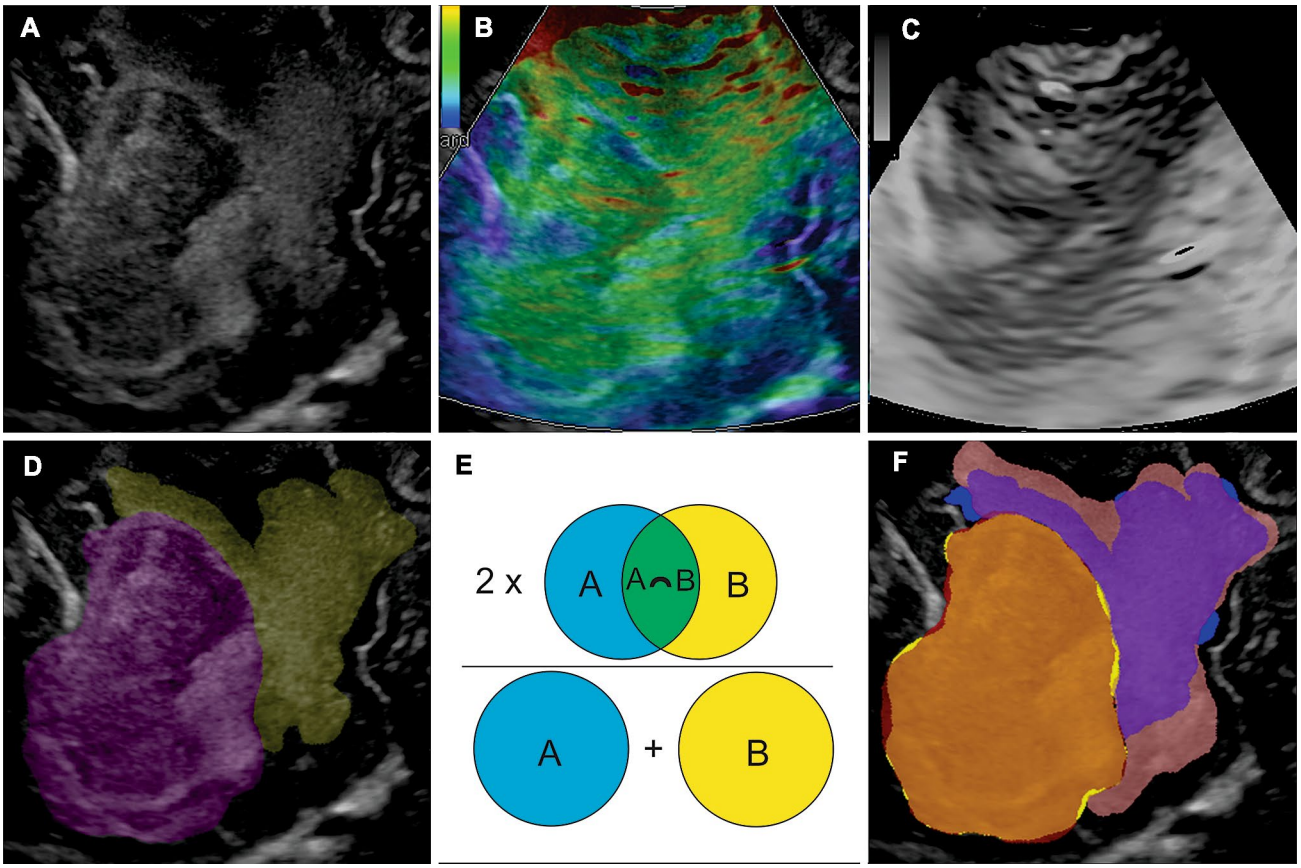

Fig. 2 Example of intraoperative ultrasound images and manual segmentation technique. **a** Image of B-mode. **b** Image of the elastogram. According to the colour code, the softest tissues appear in green and the hardest in blue. **c** Hue component of the elastogram image. **d** Illustrative case of the segmentation of the tumour (purple) and peritumoural region (yellow). **e** Illustration of the Sorensen–Dice coefficient. The blue circle represents the reference ROI, and the yellow circle represents the ROI drawn by a second observer. In green is the overlap area. **f** Example of the concordance visualisation between two segmentations. The overlap of the tumoural ROIs (orange) represents an excellent agreement, while the overlap of the peritumoural ROIs (purple) shows a wide variability

pixels of the evaluated ROI, and *C* is the number of pixels of the overlap area between ROIs *A* and *B* (Fig. 2e–f).

In a previous step, the images were pre-processed by resampling at 1×1 mm size, a median filter was applied to reduce noise, and the histogram's intensities were normalised. Intensity discretisation was also carried out using 256 grey levels and a relative rescaling of intensities using the three-sigma method (± 3 standard deviations [SD]). The next step was to extract the radiomic features of the segmented regions in both B-mode and elastography. Intensity and texture features are detailed in Supplementary Table 1.

Statistical analysis

All radiomic features were standardised. Correlation of OS with radiomic features was tested using Spearman's rho coefficient, which was selected to ensure all potential monotonic correlations. We removed redundant texture features with linear correlation. Thus, only a small number of the highest-ranking features were selected. For survival analysis, we determined the optimal cutpoint of the statistically significant radiomic features to split the data into high- and low-risk groups using the cutp function for the survMisc R package. The Kaplan–Meier survival curves of the two risk groups were then plotted with log-rank tests to compare the curves.

Moreover, the association of radiomic features with OS was assessed with a univariate Cox regression. The univariate prognostic performance of each feature measure was assessed using the Harrell concordance index (C-index). All statistical analyses were performed using R version 3.5.0 (R Core Team, Vienna, Austria).

Results

During the study period, a total of 25 patients with glioblastomas underwent surgery. Three patients without an IOUS study were excluded. Six patients were excluded, because

they had undergone partial resections/biopsies or they were recurrences.

A total of 16 patients were available for analysis. Thirteen (81%) were males, and three (19%) were females. The mean age was 65.5 ± 9.26 years. The median pre-operative Karnofsky Performance Scale (KPS) was 80 (interquartile range [IQR] = 10). The median pre-operative tumour volume was 16 cm^3 (IQR = 31.5). All cases were isocitrate dehydrogenase (IDH) mutant.

The results of the evaluation of semantic segmentations are summarised in Supplementary Table 2. The DSC for the tumour region had a median value of 0.9 (IQR = 0.09), while that for the peritumoural region was 0.56 (IQR = 0.35).

Because of the wide variability in the peritumoural area segmentation, these radiomic characteristics were not included in the correlation analysis with OS.

From the tumour region analysis, 52 radiomic features were obtained in each modality (B-mode and elastography) (Supplementary Table 3). The features that were best correlated with the OS were computed for each US modality. A correlation matrix of these texture features was generated to perform a collinearity diagnosis (Fig. 3). Radiomic features that were highly correlated ($r > 0.8$) were eliminated. As a result, in B-mode, conventional mean and the grey-level zone length matrix/short-zone low grey-level emphasis (GLZLM_SZLGE) showed a strong negative significant correlation with OS: $r\,(14) = -0.70$; $p = 0.003$ and $r\,(14) = -0.62$; $p = 0.012$, respectively. In the elastography modality, the grey-level zone length matrix/long-zone high grey-level emphasis (GLZLM_LZHGE) showed a moderate negative and significant correlation with OS, $r\,(14) = 0.52$; $p = 0.038$. Initial tumour volume also showed a negative and significant correlation with OS, $r\,(14) = 0.62$; $p = 0.012$.

The results of the Cox univariate analysis are summarised in Table 1. Neither age nor KPS was significantly correlated to OS in the univariate analysis. In B-mode, the variable conventional intensity mean and GLZLM_SZLGE were significantly associated with survival (hazard ratio [HR] = 2.84, confidence interval [CI] = 1.42–5.69, $p = 0.003$ and HR = 3.59, CI 1.48–8.69; $p = 0.005$.

For elastography, the GLZLM_LZHGE was significantly associated with survival (HR = 2.31, CI 1.16–4.58; $p = 0.017$). Also, pre-operative tumour volume was significantly associated with OS (HR = 1.06, CI 1.02–1.10; $p = 0.003$).

Using the radiomic features, a cut-off point was established to divide the sample into high- and low-risk survival groups (Table 2).

Each group's survival probability was estimated using Kaplan–Meier curves. The survival distributions for the three radiomic features were statistically significantly different. For conventional mean χ^2 16.5 (1), $p < 0.001$; for GLZLM_SZLGE χ^2 14.9 (1), $p < 0.001$; and for GLZLM_LZHGE, χ^2 8.4 (1), $p = 0.004$ (Fig. 4).

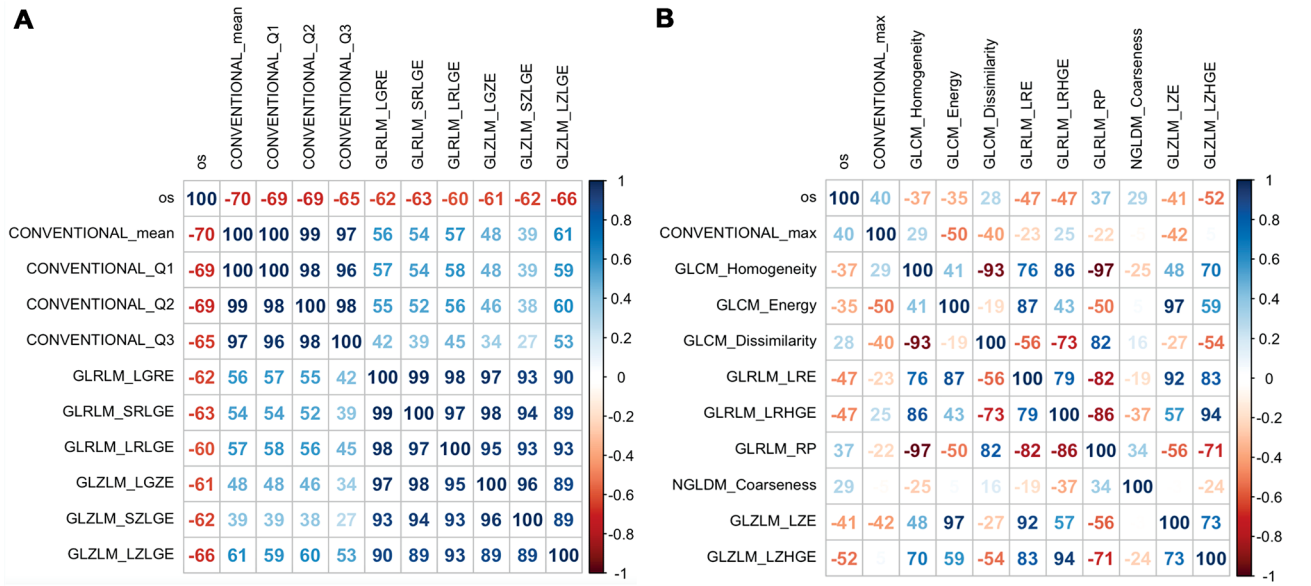

Fig. 3 Correlation matrix between the best ranked radiomic features and overall survival. **a** B-mode and **b** strain elastography. Inside the squares, the value of the Spearman coefficient appears in percentage format, as well as the colour scale representing the strength of the correlation

Table 1 Univariate Cox regression for overall survival

Variable	β	HR	95% CI	p	Likelihood ratio test	C-index
Age	0.01	1.01	0.94–1.08	0.77	$\chi^2=0.08$, $df=1$, $p=0.8$	0.46
KPS	−0.05	0.95	0.85–1.06	0.333	$\chi^2=0.97$, $df=1$, $p=0.3$	0.58
Initial tumor volume	0.06	1.06	1.02–1.10	0.003	$\chi^2=10.62$, $df=1$, $p=0.001$	0.80
B-mode						
Conventional mean	1.04	2.84	1.42–5.69	0.003	$\chi^2=9.31$, $df=1$, $p=0.002$	0.85
GLZLM_SZLGE	1.28	3.59	1.48–8.69	0.005	$\chi^2=0.48$, $df=1$, $p=0.002$	0.75
Strain elastography						
GLZLM_LZHGE	0.84	2.31	1.16–4.58	0.017	$\chi^2=5.02$, $df=1$, $p=0.02$	0.61

HR hazard ratio, *KPS* Karnofsky Performance Score, *GLZLM_SZLGE* coventional intensity mean and the grey-level zone length matrix/short-zone low gray-level emphasis, *GLZLM_LZHGE* grey-level zone length matrix/long-zone high gray-level emphasis

Table 2 Kaplan–Meier analysis for overall survival and texture-based groups

Radiomic feature	Cutpoint	Risk groups and number of cases	Median OS (IQR)	Log-rank test	
				χ^2	p
Conventional mean	−0.1824347	Low = 8	427 (197)	16.5	< 0.001
		High = 8	126 (114)		
GLZLM_SZLGE	−0.1300415	Low = 12	374 (182)	14.9	< 0.001
		High = 4	106 (50)		
GLZLM_LZHGE	0.2890771	Low = 13	361 (175)	8.4	0.004
		High = 3	109 (86)		

OS overall survival, *IQR* interquartile range, *GLZLM_SZLGE* coventional intensity mean and the grey-level zone length matrixshort-zone low gray-level emphasis, *GLZLM_LZHGE* grey-level zone length matrix/long-zone high gray-level emphasis

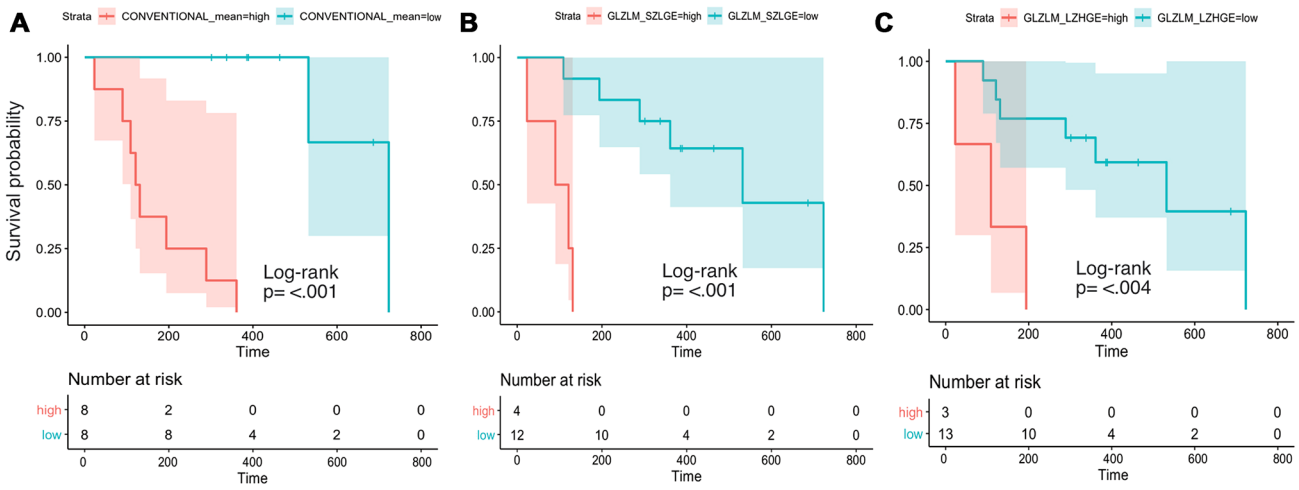

Fig. 4 Survival probability estimated by the Kaplan–Meier curves, including 95% confidence intervals. Censoring is indicated by vertical marks. Statistical significance was calculated by the log-rank test. The comparison groups correspond to the variables: conventional mean (**a**) and GLZLM_ SZLGE (**b**) from B-mode and GLZLM_ LZHGE (**c**) from strain elastography

Discussion

This feasibility study found a significant correlation between tumour radiomic characteristics of intraoperative ultrasound B-mode and strain elastography with OS in glioblastomas.

Among the strengths of our work, we can say that to the best of our knowledge, this is the first study to implement quantitative texture analysis of IOUS images in both B-mode and strain elastography in brain tumours. This study is also the first to attempt to correlate the radiomic features of IOUS images with the OS of brain tumour patients.

On the other hand, we verified that the segmentation method is sufficiently consistent and accurate to delimit the tumour areas, but not peritumoural areas. Although limited, our sample is homogeneous, since all patients underwent surgery using the same surgical technique (performing complete resections in all cases) and received the same treatment protocol. Furthermore, both the US equipment and the parameters used to acquire the intraoperative images were the same in all cases.

Advanced image processing and artificial intelligence intervention have made great strides in characterising brain tumours and developing predictive models of survival and response to treatment [21]. Preoperative MRI images have proven to provide valuable information for elaborating such models; however, the difficulty in harmonisation and variability between processing pipelines continues to be a challenge [22].

Even though image quality and resolution could be considered inferior compared with other imaging techniques such as MRI, there is growing evidence that the US image contains biological information that can be set as a base to create models that allow classification tasks, for example, benignity versus malignancy [23]. Also, the capacity of US as a prognostic marker in response to adjuvant treatments in breast pathology has recently been evaluated [24, 25]. One possible explanation may lie in the fact that echogenicity in B-mode and loss of elasticity identified by IOUS-E could be associated with cellularity, which, on the other hand, is related to tumour aggressiveness.

The main limitation of US is the dependence on the explorer and the variability between the parameters used in image acquisition among different centres. For this reason, image pre-processing is a fundamental step [26].

IOUS imaging facilitates tumour resection, and these images can be used to create a radiomic profile that provides information about the survival and progression of these tumours. We emphasise the simplicity of the processing and extraction of radiomic variables using a series of user-friendly and open source programs.

We are aware of the study limitations, such as the small sample size and low representativeness of the entire tumour volume when basing the analysis on a single image. Another disadvantage is the lack of an integration tool in our navigation system for US and pre-operative MRI. For this reason, segmentation of peritumoural areas is particularly complicated, since there was no 'ground truth' from a reference imaging technique, such as MRI. For this reason, since this is an initial study, it seemed correct to use only the tumour region. On the other hand, the statistical analysis is limited to the univariate correlations between radiomic characteristics and survival. Given our sample size, it seemed inappropriate to perform multivariate analysis, much less a predictive model, in the absence of a validation cohort.

Besides providing better contrast to distinguish tumour morphology, intra-operative elastography can contain important information about cytoarchitecture and biological behaviour. This information, in turn, may have prognostic implications in these patients.

Our results may serve as the basis for future multi-institutional studies to validate the relationship between the quantitative analysis of intra-operative US images and the prognosis of patients with glioblastoma diagnosis, integrating these findings with other available sources at the time, such as the case of the presurgical MRI.

Conclusion

According to our results, quantitative texture analysis of intra-operative B-mode US and strain elastography is feasible in glioblastomas. The radiomic characteristics of the tumour region correlate with the OS of these patients.

Supplementary Information The online version contains supplementary material available at https://doi.org/10.1007/s40477-021-00569-9.

Acknowledgements We thank all the members of the Radiology Department of our hospital for their support in carrying out this work.

Author contributions All authors contributed to the study conception and design. Material preparation, data collection and analysis were performed by SG-G, RS, MV-C and IA. The first draft of the manuscript was written by SC and all authors commented on previous versions of the manuscript. All authors read and approved the final manuscript.

Funding No funding was received for this research.

Data availability The data that support the findings of this study are available from the corresponding author upon reasonable request.

Compliance with ethical standards

Conflict of interest All authors certify that they have no affiliations with or involvement in any organization or entity with any financial interest (such as honoraria; educational grants; participation in speakers' bureaus; membership, employment, consultancies, stock ownership,

or other equity interest; and expert testimony or patent-licensing arrangements), or non-financial interest (such as personal or professional relationships, affiliations, knowledge or beliefs) in the subject matter or materials discussed in this manuscript.

Ethical approval All procedures performed in studies involving human participants were in accordance with the ethical standards of the Ethics Committee of our center and with the 1964 Helsinki declaration and its later amendments or comparable ethical standards.

Informed consent Informed consent was obtained from all individual participants included in the study.

References

1. Koshy M, Villano JL, Dolecek TA et al (2012) Improved survival time trends for glioblastoma using the SEER 17 population-based registries. J Neurooncol 107:207–212. https://doi.org/10.1007/s11060-011-0738-7
2. Kickingereder P, Neuberger U, Bonekamp D et al (2018) Radiomic subtyping improves disease stratification beyond key molecular, clinical, and standard imaging characteristics in patients with glioblastoma. Neuro Oncol 20:848–857. https://doi.org/10.1093/neuonc/nox188
3. Bakas S, Shukla G, Akbari H et al (2020) Overall survival prediction in glioblastoma patients using structural magnetic resonance imaging (MRI): advanced radiomic features may compensate for lack of advanced MRI modalities. J Med imaging (Bellingham, Wash) 7:031505. https://doi.org/10.1117/1.JMI.7.3.031505
4. Sastry R, Bi WL, Pieper S et al (2017) Applications of ultrasound in the resection of brain tumors. J Neuroimaging 27:5–15. https://doi.org/10.1111/jon.12382
5. Del Bene M, Perin A, Casali C et al (2018) Advanced ultrasound imaging in glioma surgery: beyond gray-scale B-mode. Front Oncol. https://doi.org/10.3389/fonc.2018.00576
6. Prada F, Del Bene M, Rampini A et al (2019) Intraoperative strain elastosonography in brain tumor surgery. Oper Neurosurg 17:227–236. https://doi.org/10.1093/ons/opy323
7. Della Pepa GM, Ius T, La Rocca G et al (2020) 5-Aminolevulinic acid and contrast-enhanced ultrasound: the combination of the two techniques to optimize the extent of resection in glioblastoma surgery. Neurosurgery 86:E529–E540. https://doi.org/10.1093/neuros/nyaa037
8. Selbekk T, Bang J, Unsgaard G (2005) Strain processing of intraoperative ultrasound images of brain tumours: Initial results. Ultrasound Med Biol 31:45–51. https://doi.org/10.1016/j.ultrasmedbio.2004.09.011
9. Unsgaard G, Ommedal S, Muller T et al (2002) Neuronavigation by intraoperative three-dimensional ultrasound: initial experience during brain tumor resection. Neurosurgery 50:804–812. https://doi.org/10.1097/00006123-200204000-00022
10. Prada F, Del Bene M, Mattei L et al (2014) Fusion imaging for intra-operative ultrasound-based navigation in neurosurgery. J Ultrasound 17:243–251. https://doi.org/10.1007/s40477-014-0111-8
11. Vitale V, Rossi E, Di Serafino M et al (2020) Pediatric encephalic ultrasonography: the essentials. J Ultrasound 23:127–137. https://doi.org/10.1007/s40477-018-0349-7
12. Bhatia KSS, Tong CSL, Cho CCM et al (2012) Shear wave elastography of thyroid nodules in routine clinical practice: preliminary observations and utility for detecting malignancy. Eur Radiol 22:2397–2406. https://doi.org/10.1007/s00330-012-2495-1
13. Ferraioli G, Parekh P, Levitov AB, Filice C (2014) Shear wave elastography for evaluation of liver fibrosis. J Ultrasound Med 33:197–203. https://doi.org/10.7863/ultra.33.2.197
14. Berg WA, Cosgrove DO, Doré CJ et al (2012) Shear-wave elastography improves the specificity of breast US: the BE1 multinational study of 939 masses. Radiology 262:435–449. https://doi.org/10.1148/radiol.11110640
15. Chauvet D, Imbault M, Capelle L et al (2015) In vivo measurement of brain tumor elasticity using intraoperative shear wave elastography. Ultraschall der Medizin Eur J Ultrasound 37:584–590. https://doi.org/10.1055/s-0034-1399152
16. Cepeda S, Barrena C, Arrese I et al (2020) Intraoperative ultrasonographic elastography: a semi-quantitative analysis of brain tumor elasticity patterns and peritumoral region. World Neurosurg 135:e258–e270. https://doi.org/10.1016/j.wneu.2019.11.133
17. Stupp R, Mason WP, van den Bent MJ et al (2005) Radiotherapy plus concomitant and adjuvant temozolomide for glioblastoma. N Engl J Med 352:987–996. https://doi.org/10.1056/NEJMoa043330
18. Chakraborty A (2007) The developement of intraoperative ultrasound elasticity imaging techniques to assist during brain tumour resection. Doctoral thesis. University of London.
19. Nioche C, Orlhac F, Boughdad S et al (2018) LIFEx: a freeware for radiomic feature calculation in multimodality imaging to accelerate advances in the characterization of tumor heterogeneity. Cancer Res 78:4786–4789. https://doi.org/10.1158/0008-5472.CAN-18-0125
20. Dice LR (1945) Measures of the amount of ecologic association between species. Ecology 26:297–302. https://doi.org/10.2307/1932409
21. Rudie JD, Rauschecker AM, Bryan RN et al (2019) Emerging applications of artificial intelligence in neuro-oncology. Radiology 290:607–618. https://doi.org/10.1148/radiol.2018181928
22. Carré A, Klausner G, Edjlali M et al (2020) Standardization of brain MR images across machines and protocols: bridging the gap for MRI-based radiomics. Sci Rep 10:1–15. https://doi.org/10.1038/s41598-020-69298-z
23. Zhou H, Jin Y, Dai L et al (2020) Differential diagnosis of benign and malignant thyroid nodules using deep learning radiomics of thyroid ultrasound images. Eur J Radiol 127:108992. https://doi.org/10.1016/j.ejrad.2020.108992
24. Quiaoit K, DiCenzo D, Fatima K et al (2020) Quantitative ultrasound radiomics for therapy response monitoring in patients with locally advanced breast cancer: multi-institutional study results. PLoS ONE 15:1–19. https://doi.org/10.1371/journal.pone.0236182
25. Dasgupta A, Brade S, Sannachi L et al (2020) Quantitative ultrasound radiomics using texture derivatives in prediction of treatment response to neo-adjuvant chemotherapy for locally advanced breast cancer. Oncotarget 11:3782–3792. https://doi.org/10.18632/oncotarget.27742
26. Perez-Moreno A, Dominguez M, Migliorelli F et al (2019) Clinical feasibility of quantitative ultrasound texture analysis: a robustness study using fetal lung ultrasound images. J Ultrasound Med 38:1459–1476. https://doi.org/10.1002/jum.14824

Publisher's Note Springer Nature remains neutral with regard to jurisdictional claims in published maps and institutional affiliations.